Acta Crystallographica Section B
Structural Science
ISSN 0108-7681

The crystal structure of $Zr_2NiD_{4.5}$

M. H. Sørby,[a]* A. E. Gunnæs,[b] O. M. Løvvik,[a,c] H. W. Brinks,[a] H. Fjellvåg[c] and B. C. Hauback[a]

[a]Institute for Energy Technology, PO Box 40, NO-2027 Kjeller, Norway, [b]Department of Physics, University of Oslo, PO Box 1048 Blindern, NO-0316 Oslo, Norway, and [c]Centre for Material Science and Nanotechnology, PO Box 1126 Blindern, NO-0318 Oslo, Norway

Correspondence e-mail: magnuss@ife.no

Received 10 April 2006
Accepted 2 August 2006

The crystal structure of $Zr_2NiD_{4.5}$ has been determined by a combination of synchrotron radiation powder X-ray diffraction, electron diffraction and powder neutron diffraction data. Deuterium ordering results in a triclinic supercell given by $a_{super} = 6.81560\ (7)$, $b_{super} = 8.85137\ (9)$, $c_{super} = 8.88007\ (10)$ Å, $\alpha_{super} = 79.8337\ (8)$, $\beta_{super} = 90.0987\ (9)$, $\gamma_{super} = 90.3634\ (9)^\circ$, which relates to the non-super unit cell as $\mathbf{a}_{super} = -\mathbf{a}$, $\mathbf{b}_{super} = -\mathbf{b} - \mathbf{c}$, $\mathbf{c}_{super} = -\mathbf{b} + \mathbf{c}$. The centrosymmetric and fully ordered deuterium sublattice was determined by simulated annealing and Rietveld refinement. Deuterium was found to occupy three types of tetrahedral sites: two that are coordinated by four Zr atoms and one that is coordinated by three Zr atoms and one Ni atom. All D—D distances are longer than 2 Å. The feasibility of the crystal structure was supported by density functional theory calculations.

1. Introduction

Zr_2Ni (tetragonal, Al_2Cu-type structure, space group $I4/mcm$) absorbs deuterium to the composition $Zr_2NiD_{\sim 5}$ (Chikdene, Baudry, Boyer *et al.*, 1989; Aubertin & Campbell, 1990). Unlike other known hydride-forming Al_2Cu-type intermetallics (Bonhomme *et al.*, 1993; Yartys, Fjellvåg, Hauback & Riabov, 1998; Vennström & Andersson, 2004; Sørby *et al.*, 2000), Zr_2Ni loses the tetragonal symmetry upon deuteration. $Zr_2NiD_{4.2}$ has a slight monoclinic deformation ($a \simeq b \neq c$, $\beta = 91^\circ$, space group $I2/c$), and a partly ordered deuterium sublattice (Elcombe *et al.*, 1996). Chikdene, Baudry, Boyer *et al.* (1989) observed unindexed powder neutron diffraction (PND) peaks for $Zr_2NiD_{4.8}$ and suggested an orthorhombic supercell as a result of deuterium ordering. However, the crystal structure was not determined. A recent synchrotron radiation powder X-ray diffraction (SR-PXD) study revealed a slight triclinic deformation of the metal lattice of $Zr_2NiD_{4.8}$ (Sørby *et al.*, 2005).

The present work aims to determine the crystal structure of saturated Zr_2Ni deuteride.

Zr_2Ni contains four types of tetrahedral interstices that are candidates for deuterium occupation. Two of them, with Wyckoff positions 16(l) and 4(b), are coordinated by four Zr atoms. The 32(m) site is coordinated by three Zr and one Ni atoms, and 16(k) is coordinated by two Zr and two Ni atoms. The interstices and their interrelations are discussed in more detail by Sørby *et al.* (2005).

2. Experimental

Zr_2Ni was prepared by arc-melting a stoichiometric mixture of the elements (Goodfellow 99.99% Ni and Metron Inc. 99.95% Zr) under argon atmosphere. The sample was turned and

remelted several times and subsequently annealed at 1073 K for 23 h under vacuum in a stainless steel autoclave to increase homogeneity.

The intermetallic was deuterated in a Sieverts-type apparatus. Deuterium was used rather than natural hydrogen because of the high incoherent neutron scattering cross section of the latter. The deuterium absorption was very fast, and a starting pressure of around 0.1 bar and ice–water cooling was used to avoid overheating and disproportionation of the sample (van Essen & Buschow, 1979). A final pressure slightly above 1 bar was used for saturation. The volumetrically determined composition was $Zr_2NiD_{4.8\,(1)}$.

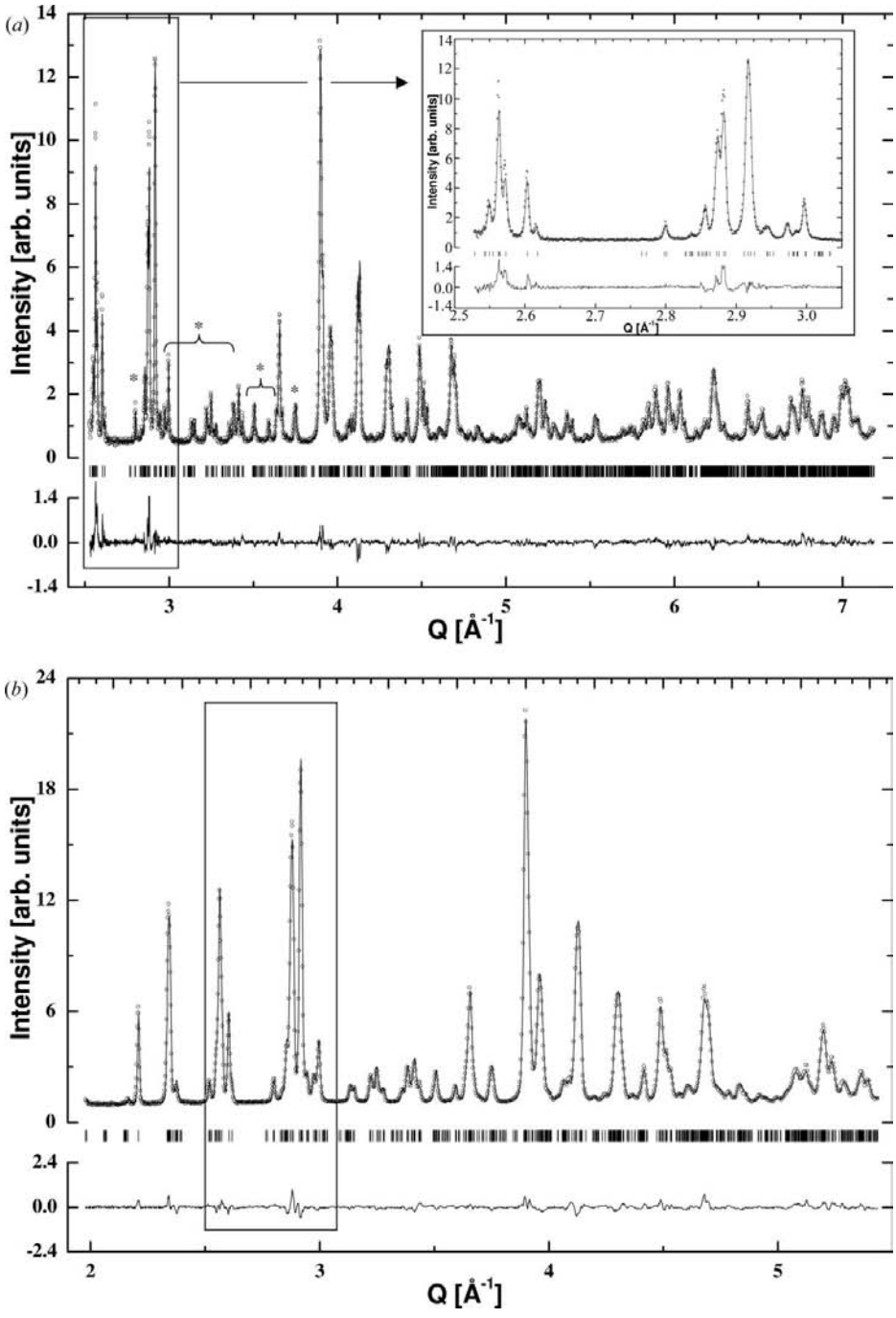

Figure 1
Rietveld fits to (*a*) HRPD backscattering data and (*b*) HRPD 90° data from $Zr_2NiD_{4.5}$ obtained by simultaneous Rietveld refinement in *GSAS* showing observed (circles), calculated (solid line) and difference plots (below). R_{wp} = 0.0599 and 0.0369, respectively. Peaks due to deuterium ordering are marked with asterisks in (*a*). The intensity mismatch discussed in the text is shown inset in (*a*). The same peaks in the 90° data are boxed in (*b*) for comparison. The data are plotted as a function of Q (= $2\pi/d$) for easy comparison.

Powder neutron diffraction data were collected at the time-of-flight (TOF) instrument HRPD at ISIS, Didcot, UK (Ibberson *et al.*, 1992). HRPD features an almost 100 m flight path resulting in superb resolution. Detectors are placed in backscattering position (2θ = 168°) and at 2θ = 90°. The best resolution is obtained in backscattering where the instrumental $\Delta d/d$ is about 4×10^{-4} in the whole measurement range. The sample was kept in a 7 mm vanadium can at ambient temperature (298 K) during the measurement.

Transmission electron microscopy (TEM) samples were prepared by leaving droplets of ethanol with a finely dispersed sample to dry on Cu grids with holey carbon films. The TEM study was performed in an analytical Jeol 2000FX microscope operating at 200 kV. A double tilt holder with allowed tilting angles of up to ± 25 and ± 46° was used. Tilting series were performed in the transmission electron microscope in order to locate the position of both strong and weak reflections in the reciprocal space, making it possible to construct the complete reciprocal lattice of the structure.

Pressure–composition isotherms were measured in an in-house built, fully automated Sieverts-type apparatus. The instrument is equipped with two pressure transducers: a Baratron MKS120 (accuracy 0.08% of reading; supplier's calibration) which operates from 0 to 28 bar and a Presens transducer (accuracy ±4 mbar; calibrated against a dead-weight tester) primarily for the range 28–100 bar. The equilibrium criterion was set to $dp/dt \leq 2$ mbar h^{-1}. The sample was kept in an SS316L sample holder. Approximately 4 ml of the sample holder was heated to 323 K, while the remaining system was 313 K in two heating cabinets with temperature stabilities of ±0.02 and

±0.05 K. The total system volume was 50 ml. The H_2 compressibilites of Hemmes *et al.* (1986) were used in the calculations.

Density-functional band-structure calculations were carried out using the Vienna *Ab-initio* Simulation Package (*VASP*) (Kresse & Hafner, 1993; Kresse & Furthmüller, 1996). The projector augmented-wave method (Blöchl, 1994; Kresse & Joubert, 1999) was used to represent the valence electron density, and the exchange-correlation potential was in the generalized gradient approximation (Perdew *et al.*, 1992). The criterion for self-consistency was that two consecutively calculated energies differed by less than 0.01 meV. The plane-wave cutoff energy was 780 eV, and the spacing of **k** points was below 0.2 $Å^{-1}$. The overall convergence of the calculated total energy was of the order of 1 meV. Relaxation of the structure was performed using the residual minimization method with direct inversion in iterative subspace, which is an implementation of the quasi-Newton method. Convergence of the structure was defined to be when all the forces were smaller than 0.05 eV $Å^{-1}$.

The deuterium distribution was modelled by simulated annealing based on the PND data with the program *RMCPOW* (Mellergård & McGreevy, 2001). The metal atoms were kept fixed at the positions determined by SR-PXD (Sørby *et al.*, 2005) and the D atoms were randomly distributed over the tetrahedral sites in the model in accordance with the nominal composition. Atoms with zero scattering power (representing vacancies) were placed in the rest of the tetrahedral sites. A random D atom and a random 'vacancy' were allowed to swap positions. The swap was accepted if it improved the agreement between the observed and calculated PND data. Otherwise, it was rejected with a probability that increased exponentially with the degree of deterioration of the agreement. New swaps were tested and accepted/rejected until there was no further improvement in the fit between the observed and calculated data.

Rietveld refinement was performed with the program *GSAS* (Larson & Von Dreele, 1994) with the *EXPGUI* graphical interface (Toby, 2001). The TOF profiles were modelled by the Ikeda–Carpenter function convoluted with a pseudo-Voigt function (three refinable parameters). Backgrounds were modelled with shifted Chebyshev polynomials with 12 parameters. Le Bail refinements (*i.e.* 'structureless refinements') were performed according to the description of Le Bail *et al.* (1988).

3. Results and discussion

SR-PXD showed a single triclinic phase with unit-cell parameters a = 6.81744 (8), b = 6.80177 (8), c = 5.69042 (4) Å, α = 90.191 (1), β = 90.200 (1), γ = 90.2886 (8)°, as reported by Sørby *et al.* (2005). The PND data contained several reflections that are inconsistent with this unit cell, thus indicating that the D atoms form a superlattice in accordance with the findings of Chikdene, Baudry, Boyer *et al.* (1989) (Fig. 1*a*). However, owing to the lack of low-Q ordering reflections, it was virtually impossible to determine the supercell from the PND data alone.

The ordering was therefore further investigated by electron diffraction (ED) using TEM, where very weak ordering reflections can be observed owing to the strong interactions between electrons and solid matter. The [001] projection can be fully indexed according to the X-ray unit cell. The [100] projection, on the other hand, contains two sets of ordering reflections (described as weak and very weak) with half-integer k and l index, *e.g.* $0\frac{1}{2}\frac{1}{2}$ and $0\frac{3}{2}\frac{3}{2}$, respectively (Fig. 2). Several other projections were measured in tilt series so that the whole reciprocal lattice could be constructed. All peaks could be indexed as h k/2 l/2. This result indicates that the ordering takes place in the *bc* plane, while there is no change of periodicity along the *a* axis. The smallest supercell that is consistent with the observed TEM reflections is obtained with the new *c* axis as the cell diagonal of the former *bc* plane (keeping the *a* and *b* axes unchanged), thus transforming $0\frac{1}{2}\frac{1}{2}$ to 001. However, this supercell is unable to account for the majority of the ordering peaks observed by PND. A supercell of twice the size is obtained with both the *b* and the *c* axis as cell diagonals of the former *bc* plane: $\mathbf{a}_{super} = -\mathbf{a}$, $\mathbf{b}_{super} = -\mathbf{b} - \mathbf{c}$, $\mathbf{c}_{super} = -\mathbf{b} + \mathbf{c}$. A Le Bail refinement showed that this supercell, which is twice as large as the X-ray unit cell, is in very good agreement with the PND data and it was thus used for simulated annealing.

Simulated annealing was performed with the backscattering HRPD data and 39 D atoms (corresponding to the composition $Zr_2NiD_{4.88}$) in the supercell. The swapping was performed under the constraint that the D—D distances should be more than 2 Å, in accordance with the Switendick (1978, 1979) criterion.

The converged structure model was transferred to the Rietveld program *GSAS*. D- and metal-atom positions were refined in space group *P*1 with reasonable soft constraints on selected metal–deuterium distances (Zr—D 2.10 and Ni—D 1.62 Å). The constraints were weighted so that they were fulfilled within approximately 0.1 Å. The displacement parameters were refined as a single parameter for each element.

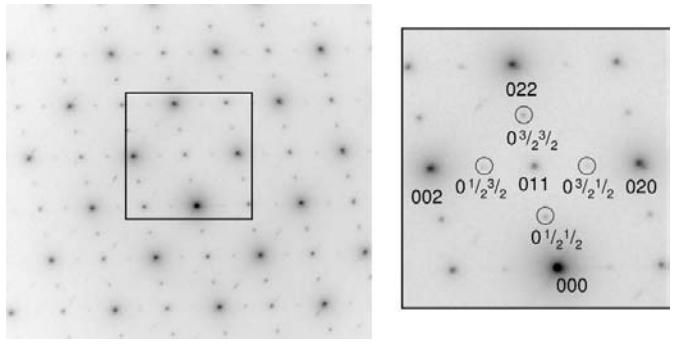

Figure 2
Electron diffraction pattern of saturated Zr_2Ni deuteride in the [100] projection. The area within the grey box is shown enlarged (right) with Miller indices according to the X-ray unit cell. Some of the weak ordering reflections are marked with black circles.

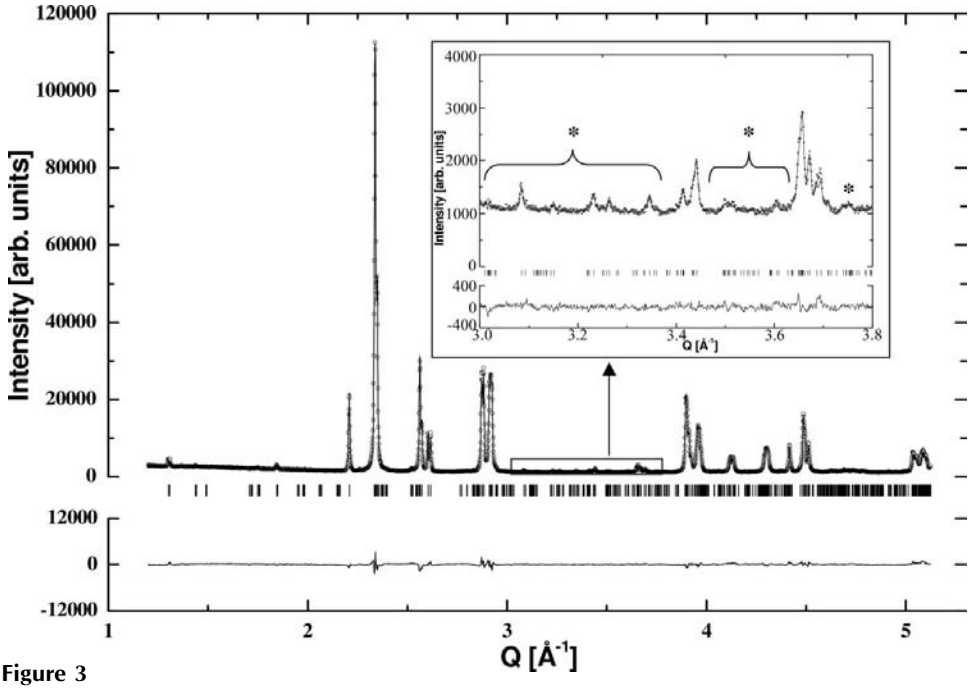

Figure 3
Agreement between previously obtained SR-PXD data (Sørby *et al.*, 2005) and the structure model for $Zr_2NiD_{4.5}$ refined from PND data. Peaks that are inconsistent with the non-super triclinic unit cell are marked with asterisks (*) in the inset. Note that the structure model is *not* refined to the SR-PXD data. R_{wp} = 0.0515, λ = 0.49956 Å.

The two data sets from HRPD were used simultaneously in the refinement. Most atoms shifted only slightly from the positions obtained by simulated annealing, but four D atoms repeatedly moved far away from the centre of the tetrahedral sites, thus engaging in unreasonably short interatomic distances. These atoms were removed from the structure model and one new D position was located by difference Fourier mapping, giving the composition $Zr_2NiD_{4.5}$ ($Zr_4Ni_2D_9$). Some reconstruction of the deuterium lattice took place in the subsequent refinement. The program *ADDSYM* (Spek, 2003) revealed that the structure model contained a pseudo-symmetry centre and was close to *B*-centred. However, the set of very weak ordering reflections observed by TEM, *e.g.* 021 (indexed as $0\frac{31}{22}$ in Fig. 2), were inconsistent with *B*-centring. Tilting series, where $0\frac{\bar{1}1}{22}$ and $0\frac{1\bar{1}}{22}$ (index according to Fig. 2) have been in the common row of reflections, show that the very weak reflections exist independently of orientation. They cannot therefore be ascribed to multiple scattering, but exist because of the lack of *B*-centring. The very low intensity of these reflections is consistent with the structure being close to *B*-centred.

The possible symmetry centre was further investigated by *density functional* band-structure calculations. The pseudo-centrosymmetric Rietveld model was first relaxed, which yielded a structure only slightly different from the starting point. The atomic arrangement had actually moved closer to true centrosymmetry, and the calculation was therefore rerun in $P\bar{1}$. The energy difference between the two structures was less than 0.01 eV per unit cell, which is below the uncertainty in such calculations (Løvvik & Swang, 2004). The resulting unit-cell parameters of the centrosymmetric model were a = 6.819, b = 8.862, c = 8.908 Å, α = 80.13 , β = 89.87, γ = 89.75°. The calculated lattice constants all differ less than 0.4% from the refined lattice constants presented in Table 1. The angles deviate somewhat from those achieved by the Rietveld refinement below, but not more than could be expected by calculations performed at 0 K and without zero-point energy corrections. The calculated coordinates differ by less than 0.01 from the refined values for most of the atoms, except two D coordinates, which differ by 0.016 and 0.018. This result is also a strong support of the suggested structure model. Hence, the density functional theory calculations show that the structure model is indeed physically feasible and indicate that the crystal structure is truly centrosymmetric.

The final Rietveld refinement was, on the basis of the results above, carried out in the space group $P\bar{1}$. The refinement is summarized in Table 1 and the crystal structure is presented in the CIF deposited with this paper.[1] The obtained fits are in general good except in the highest TOF (lowest Q) region of the backscattering data from HRPD where a multiplet is clearly under-fitted (Fig. 1*a*). Oddly, the same multiplet is adequately fitted for the data from the 90° detector bank (Fig. 1*b*). It should be noted that there were distinct problems in the *GSAS* fit to backscattering HRPD data from a CeO_2 standard in the same high-TOF range. Thus, it is suspected that the problems are due to some shortcoming in the profile calculations rather than the structure model.

The previously obtained SR-PXD data (Sørby *et al.*, 2005) were not included in the refinement because of a slight difference in deuterium content, and thereby unit-cell dimensions, since the SR-PXD and PND measurements were carried out with some months' separation. However, to check for consistency, the PND-refined structure model was fitted to the SR-PXD data, refining only the lattice parameters, zero-point and profile shape parameters (atomic positions and displacement parameters fixed). The obtained fit was excellent (Fig. 3). Interestingly, even some minute ordering peaks, caused by the slight shifts of the metal atom, are well fitted. This agreement strongly supports the structure model obtained.

[1] Supplementary data for this paper are available from the IUCr electronic archives (Reference: LM5003). Services for accessing these data are described at the back of the journal.

Table 1
Rietveld refinement summary.

Crystal data	
Chemical formula	$D_9Ni_2Zr_4$
M_r	500.41
Cell setting, space group	Triclinic, $P\overline{1}$
a, b, c (Å)	6.81560 (7), 8.85137 (9), 8.88007 (10)
α, β, γ (°)	79.8337 (8), 90.0987 (9), 90.3634 (9)
V (Å^3)	527.290 (6)
Z	4
Radiation type	Neutron
Temperature (K)	298
Data collection	
Diffractometer	HRPD (ISIS)
Data collection methods	TOF
Measured d-value interval (Å)	3.18–0.87
Refinement	
R_p(overall), R_{wp}(overall)	0.0398, 0.0446
No. of parameters	109
No. of restraints	71

Computer programs used: *RMCPOW* (Mellergård & McGreevy, 2000), *GSAS* (Larson & Von Dreele, 1994).

50% of the 4(*b*) sites (Zr_4) are occupied by deuterium (Wyckoff positions in single quotation marks refer to the sites in Zr_2Ni with *I*4/*mcm* described above). The 4(*b*) tetrahedra form isolated chains by edge-sharing in the [0$\overline{1}$1] direction (*i.e.* parallel to the *c* axis in the SR-PXD unit cell). There is a repeating pattern of two occupied tetrahedra followed by two empty ones in each chain as shown in Fig. 4. The chains are displaced relative to each other, such that the occupied 4(*b*) tetrahedra are located in layers parallel to the *ac* plane. The 16(*l*) sites within the same layers are empty as a result of face-sharing with the occupied 4(*b*) sites. Between the occupied 4(*b*) layers, the 16(*l*) sites are occupied to the maximum possible extent without face-sharing (Fig. 5*a*). The empty 4(*b*) tetrahedra share all four faces with 16(*l*) tetrahedra, of which three are occupied by deuterium. The unoccupied 16(*l*) site shares a face with an occupied 16(*l*) tetrahedron around the adjacent 4(*b*) tetrahedra. The filling scheme of the 16(*l*) sites may alternatively be described on the basis of the chains of alternating face- and corner-sharing 16(*l*) tetrahedra in the [0$\overline{1}$1] direction. The chains are filled in two different ways (Fig.

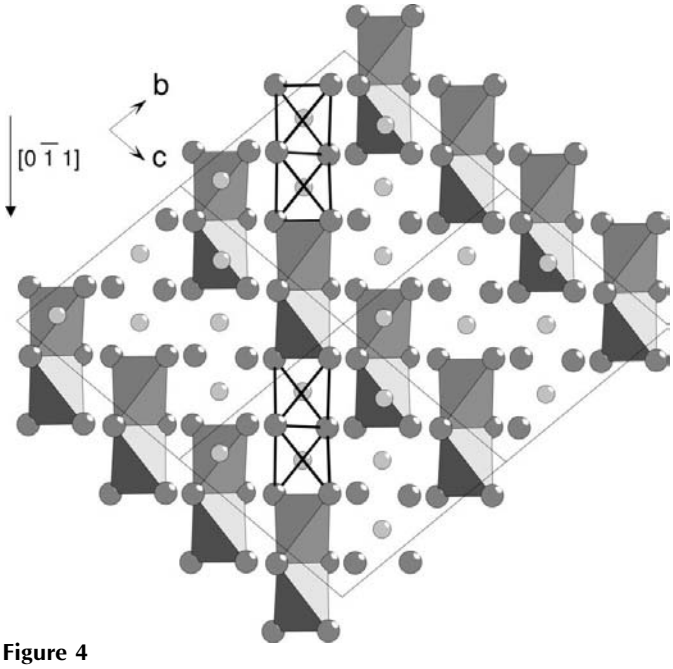

Figure 4
Occupied 4(*b*) sites (Zr_4 tetrahedra, grey) in $Zr_2NiD_{4.5}$. Zr: dark-grey spheres; Ni: light-grey spheres. Four unit cells are outlined. Some empty 4(*b*) tetrahedra are outlined (black lines) to elucidate the chains of edge-sharing 4(*b*) in the [0$\overline{1}$1] direction.

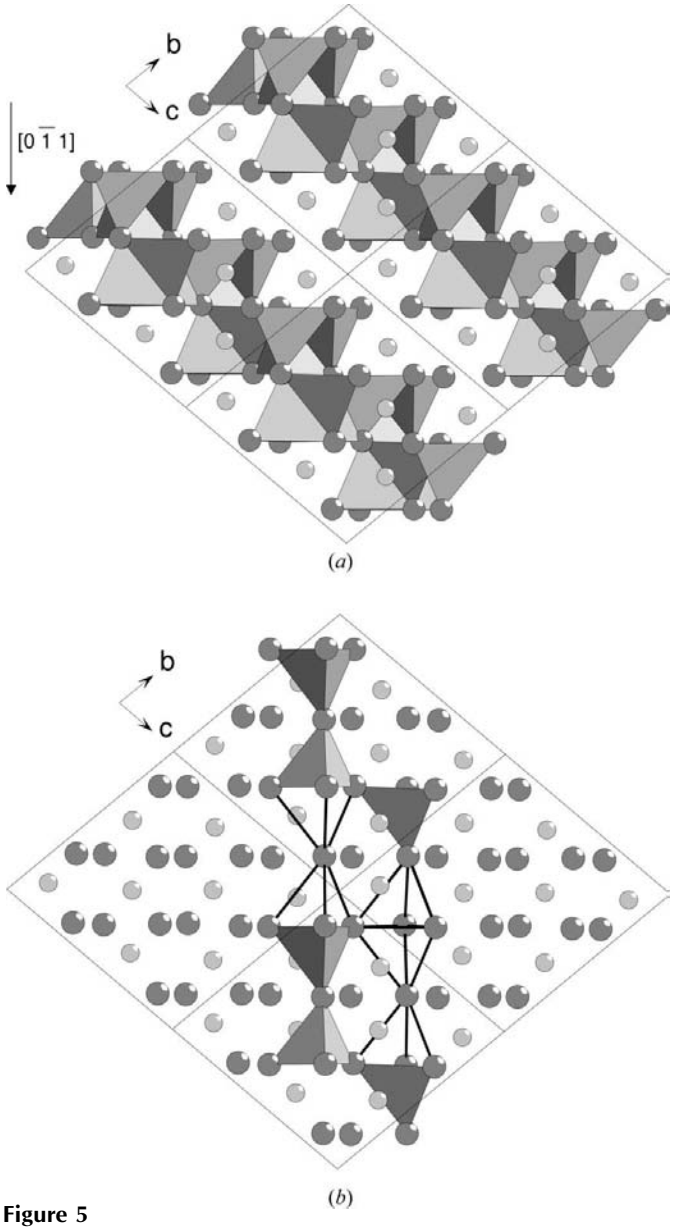

Figure 5
(*a*) Occupied 16(*l*) sites (Zr_4 tetrahedra, grey) in $Zr_2NiD_{4.5}$. Four unit cells are outlined. Zr: dark-grey spheres; Ni: light-grey spheres. (*b*) The two types of filling of the chains of alternating face- and corner-sharing 16(*l*) tetrahedra. Some empty 16(*l*) tetrahedra are outlined (black lines) to elucidate the chains of alternating face- and corner-sharing 16(*l*) tetrahedra in the [0$\overline{1}$1] direction.

5*b*). Half of the chains are 50% filled, with deuterium in every second pair of corner-sharing tetrahedra. The other half are 25% filled, with three empty sites between each occupied one. Thus, 3/8 (37.5%) of the 16(*l*) sites are occupied by deuterium.

The occupation of the 32(*m*) sites is best visualized by the deuterium coordination around the Ni atoms. Each Ni atom is coordinated by eight 32(*m*) sites. Half of the Ni atoms have two D atoms in their surrounding sites, while the rest are three-coordinated. Fig. 6(*a*) shows that three-coordinated Ni atoms occur as pairs separated by pairs of two-coordinated Ni along the chains of Ni atoms in the [0$\bar{1}$1] direction. Deuterium occupation occurs only in a subset of the 32(*m*) sites, which is given by fourfold symmetry along the Ni chains, as seen in Fig. 6(*c*).

The 32(*m*) sites are *not* occupied to the maximum extent possible without coming into conflict with the remaining sites. Only one out of the eight 32(*m*) sites around a three-coordinated Ni atom is blocked by an occupied 16(*l*) site. Since each 32(*m*) site shares two faces with other 32(*m*) sites, these Ni atoms could actually be four-coordinated by deuterium, yielding an overall composition Zr_2NiD_5 without violation of the Switendick criterion. Structure models with four-coordination were tested by Rietveld refinement; however, the resulting fits were vastly inferior to those obtained with three-coordination.

All unoccupied 4(*b*), 16(*l*) and 32(*m*) sites in $Zr_2NiD_{4.5}$ are blocked according to the Switendick criterion with the described deuterium arrangement. Still, deuterium contents higher than $Zr_2NiD_{4.5}$ are observed experimentally, as shown in the pressure–composition isotherm in Fig. 7. The isotherm shows a homogeneity range from about $Zr_2NiD_{4.4}$ to at least $Zr_2NiD_{4.9}$ [*p*(equilibrium) = 23.5 bar at 323 K] for the triclinic phase. Deuterium concentrations higher than $Zr_2NiD_{4.5}$ may be obtained by a rearrangement of the D atoms in 32(*m*) (*i.e.* a transition from three- to four-coordinated Ni as described above). Another possibility is that deuterium beyond 4.5 per formula unit is accommodated in Zr_2Ni_2 sites [16(*k*)]. The latter explanation is supported by earlier investigations. Baudry *et al.* (1990) observed highly mobile H atoms in $Zr_2NiH_{4.8}$, while the mobility of hydrogen is less in $Zr_2NiH_{4.5}$ (Aubertin *et al.*, 1987; Chikdene, Baudry & Boyer, 1989). The difference is suggested to be due to a slight filling of Zr_2Ni_2 sites in $Zr_2NiD_{4.8}$. Moreover, Chikdene, Baudry, Boyer *et al.* (1989) observed a deuterium occupation of Zr_2Ni_2 sites in disordered $Zr_2NiD_{4.8}$ at 420 K, which roughly corresponded to the increase in deuterium content above $Zr_2NiD_{4.5}$.

The refined Zr—D distances are in the range 1.98–2.22 Å, except for the distance of 2.35 (1) Å between atoms Zr6 and D6 (see CIF for atom numbering) found in a 16(*l*) tetrahedron. The distance remains abnormally long even when soft-constrained, and the fit to the experimental data deteriorates significantly if the distance is fixed to 2.2 Å [R_{wp}(o-wp(overall) increases from 0.0446 to 0.0511]. There is no obvious crystal-chemical reason for the long Zr—D distance. The remaining Zr—D distances are in fair agreement with those found in similar compounds, such as $Zr_3FeD_{6.7}$ (2.06–2.20 Å; Yartys, Fjellvåg, Hauback, Riabov & Sørby, 1998) and

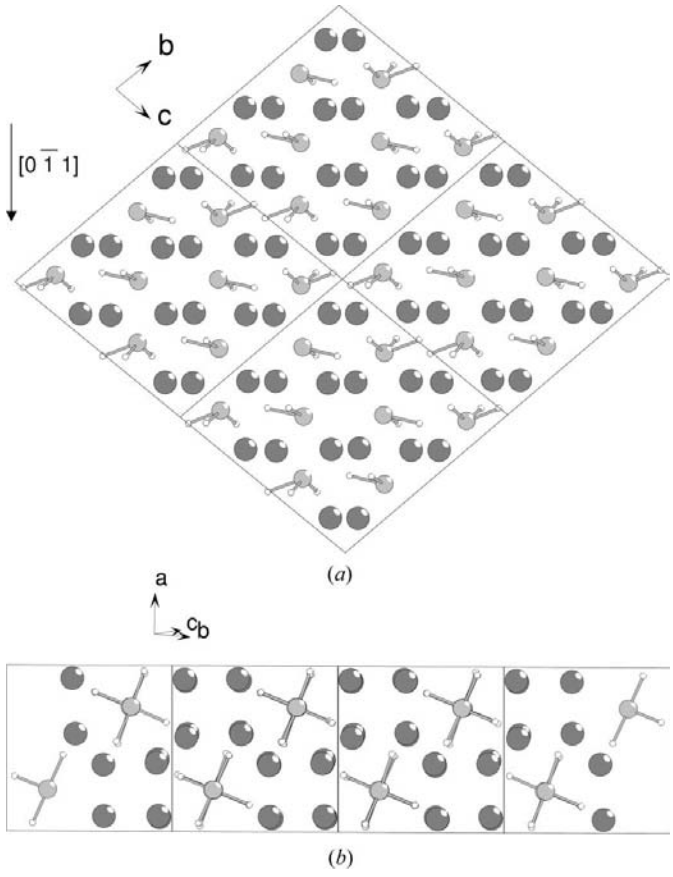

Figure 6
(*a*) An Ni—D coordination in $Zr_2NiD_{4.5}$. The D atoms are situated in 32(*m*) sites (Zr_3Ni tetrahedra). Zr: dark-grey spheres; Ni: light-grey spheres; D: white spheres. (*b*) Ni—D coordination viewed along the Ni chains ([0$\bar{1}$1] direction). Note that there is a subset of the 32(*m*) sites with fourfold symmetry around the Ni chains in which there is no D occupation.

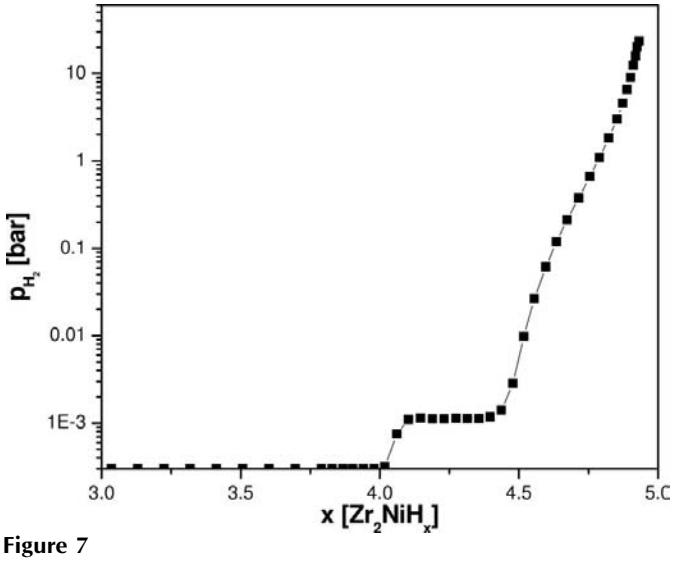

Figure 7
Pressure–composition absorption isotherm for Zr_2Ni at 323 K. Note the two-phase region between the previously reported monoclinic phase $Zr_2NiD_{4.2}$ and the trinclinic phase. Pressures below 0.3 mbar have been set to 0.3 mbar.

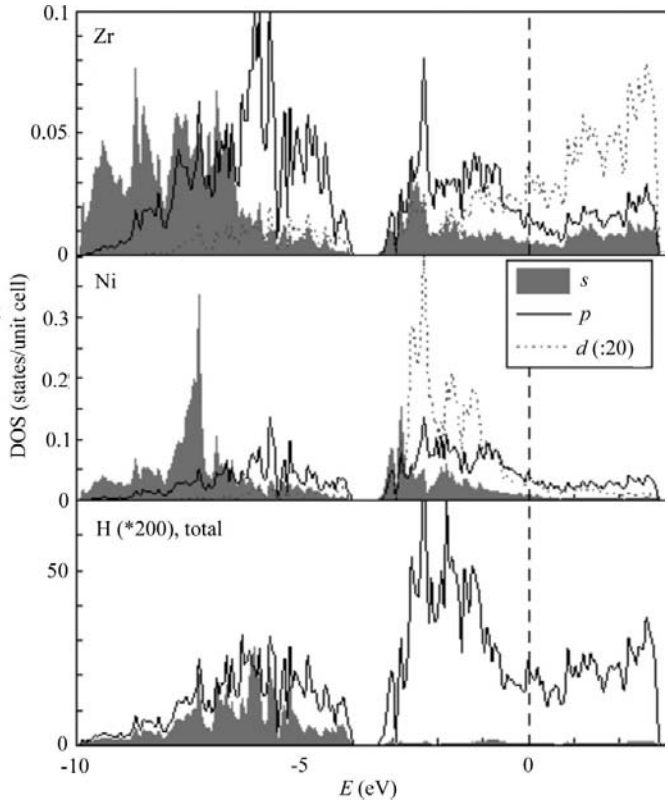

Figure 8
The local density of states projected on angular quantum numbers of the different atoms. The energy is in eV compared with the Fermi level (marked by the dashed line).

Zr_2CoD_5 (2.04–2.15 Å; Bonhomme *et al.*, 1993). The refined Ni—D distances fall in the range between 1.55 and 1.68 Å, which is in good agreement with earlier reports for *e.g.* $LaNi_5D_7$ (1.51–1.67 Å; Lartigue *et al.*, 1987). The D—Ni—D angles are between 81.8 and 91.4°. All the D—D distances are greater than 2 Å.

The bonding of the structure was investigated by calculating the local density of states (DOS), shown in Fig. 8. It is clear that $Zr_2NiD_{4.5}$ is metallic, with both Ni and Zr bands crossing the Fermi level; Zr *d* orbitals dominate the conduction band (the *d* states are plotted with a prefactor 0.05). Similarly, the upper conduction band is dominated by Ni *d* orbitals, which overlap with the Zr *d* orbitals. Thus, the overall bonding is metallic, with significant contributions from both the metals. Most of the D states, however, are below −4 eV, interacting with both Ni and Zr *spd*-hybridized orbitals. This suggests an ionic type interaction between H and its neighbouring metal atoms. This hypothesis may also be confirmed by studying the electron localization function (ELF), which exhibits strong attractors near the H atoms; elsewhere the ELF is low, designating non-localized (metallic) bonding.

Financial support from The Research Council of Norway is highly appreciated. Associate Professor Evan Gray is gratefully acknowledged for collecting PND data at HRPD (ISIS). Dr Anita Fossdal is acknowledged for her support during measurement of the pressure–composition isotherm. Dr Mark Pitt is acknowledged for his help with TOF profile functions.

References

Aubertin, F. & Campbell, S. J. (1990). *Hyperfine Interact.* **54**, 767–774.
Aubertin, F., Campbell, S. J., Pope, M. J. & Gonser, U. (1987). *J. Less-Common Met.* **129**, 297–303.
Baudry, A., Boyer, P. & Chikdene, A. (1990). *Hyperfine Interact.* **64**, 657–664.
Blöchl, P. (1994). *Phys. Rev. B*, **50**, 17953–17979.
Bonhomme, F., Yvon, K. & Zolliker, M. (1993). *J. Alloys Compd*, **199**, 129–132.
Chikdene, A., Baudry, A. & Boyer, P. (1989). *Z. Phys. Chem. Neue Folge*, **163**, 443–448.
Chikdene, A., Baudry, A., Boyer, P., Miraglia, S., Fruchart, D. & Soubeyroux, S. L. (1989). *Z. Phys. Chem. Neue Folge*, **163**, 219–224.
Elcombe, M. M., Campbell, S. J., Howard, C. J., Büttner, H. G. & Aubertin, F. (1996). *J. Alloys Compd.* **232**, 174–179.
Essen, R. M. van & Buschow, K. H. J. (1979). *J. Less-Common Met.* **64**, 277–284.
Hemmes, H., Driessen, A. & Griessen, R. (1986). *J. Phys. C*, **19**, 3571.
Ibberson, R., David, W. I. F. & Knight, K. S. (1992). Internal Report RAL-92-031. Rutherford Appleton Laboratory, Didcot, Oxford, UK.
Kresse, G. & Furthmüller, J. (1996). *Phys. Rev. B*, **54**, 11169–11186.
Kresse, G. & Hafner, J. (1993). *Phys. Rev. B*, **47**, 558–561.
Kresse, G. & Joubert, D. (1999). *Phys. Rev. B*, **59**, 1758–1775.
Larson, A. C. & Von Dreele, R. B. (1994). *GSAS*. Report No. LAUR 86-748. Los Alamos National Laboratory, New Mexico, USA.
Lartigue, C., Le Bail, A. & Percheron-Guegan, A. (1987). *J. Less-Common Met.* **129**, 65–76.
Le Bail, A., Duroy, H. & Fourquet, J. L. (1988). *Mater. Res. Bull.* **23**, 447–452.
Løvvik, O. M. & Swang, O. (2004). *Europhys. Lett.* **607**, 607–613.
Mellergård, A. & McGreevy, R. L. (2000). *Chem. Phys.* **261**, 267–274.
Mellergård, A. & McGreevy, R. L. (2001). *Mater. Sci. Forum*, **378–381**, 71–76.
Perdew, J. P., Chevary, J. A., Vosko, S. H., Jackson, K. A., Pederson, M. R., Singh, D. J. & Fiolhais, C. (1992). *Phys. Rev. B*, **46**, 6671.
Sørby, M. H., Fjellvåg, H. & Hauback, B. C. (2005). *J. Alloys Compd.* **394**, 107–112.
Sørby, M. H., Fjellvåg, H., Hauback, B. C., Maeland, A. & Yartys, V. A. (2000). *J. Alloys Compd.* **209**, 154–164.
Spek, L. A. (2003). *J. Appl. Cryst.* **36** 7–13.
Switendick, A. C. (1978). Internal Report SAND78-0250. Sandia Laboratories, New Mexico, USA.
Switendick, A. C. (1979). *Z. Phys. Chem. Neue Folge*, **117**, 89–112.
Toby, B. H. (2001). *J. Appl. Cryst.* **34**, 210–221.
Vennström, M. & Andersson, Y. (2004). *J. Alloys Compd*, **364**, 141–145.
Yartys, V. A., Fjellvåg, H., Hauback, B. C. & Riabov, A. B. (1998). *J. Alloys Compd*, **274**, 217–221.
Yartys, V. A., Fjellvåg, H., Hauback, B. C., Riabov, A. B. & Sørby, M. H. (1998). *J. Alloys Compd*, **278**, 252–259.